Symbiosis

www.symbiosisonline.org
www.symbiosisonlinepublishing.com

Research Article | Journal of Biosensors, Biomarkers and Diagnostics | Open Access

Preparation of Biocompatible Palladium-Fe_3O_4 Nanoparticles/Multiwalled Carbon Nanotubes Composite and its Electrocatalytic Activity towards Determination of Cholesterol on Screen Printed Electrode

Revanasiddappa Manjunatha[1], Gurukar S. Suresh[1, 2*], Jose S. Melo[3, 4*], Jakkid Sanetuntikul[5] and Sangaraju Shanmugam[5]

[1]*Chemistry Research Centre, S. S. M. R. V. Degree College, Jayanagar, Bangalore - 560041, India*

[2]*Department of Chemistry and Research Centre, N.M.K.R.V. College for Women, Jayangar, Bangalore -560011, India*

[3]*Nuclear Agriculture and Biotechnology Division, Bhabha Atomic Research Centre, Trombay, Mumbai - 400085, India*

[4]*Homi Bhabha National Institute, Anushakti Nagar, Mumbai- 400094, India*

[5]*Department of Energy Systems and Engineering, Daegu Gyeongbuk Institute of Science and Technology, Daegu 711-873, Republic of Korea*

Received: 03 October, 2016; Accepted: 04 January, 2017; Published: 10 February, 2017

***Corresponding authors:** Jose Savio Melo, Nuclear Agriculture and Biotechnology Division, Bhabha Atomic Research Centre, Trombay and Homi Bhabha National Institute, Anushakti Nagar, Mumbai- 400094, India, Telephone: 91 – 80 – 26654920;Fax no: 91 – 80 – 22453665;E-mail:*jsmelo@barc.gov.in

*Gurukar S. Suresh, Nuclear Agriculture and Biotechnology Division, Bhabha Atomic Research Centre, Trombay and Homi Bhabha National Institute, Anushakti Nagar, Mumbai- 400 085, India, Telephone: 91 – 22-25592760;Fax no: 91 – 22-25505151 ;E-mail:*sureshssmrv@yahoo.co.in

Abstract

A simple and facile microwave method was adopted to prepare Fe_3O_4 and Pd- Fe_3O_4 nanoparticles, which possess the mean particle diameter of 10 nm and 90 nm, respectively. Formation of Fe_3O_4 and Pd-Fe_3O_4 nanoparticles were confirmed from Powder X-ray diffraction, Transmission electron microscopy, Energy-dispersive X-ray spectroscopy, and FT-Infra red spectroscopy techniques. Negatively charged mutliwalled carbon nanotubes (COO--MWCNTs) were wrapped with positively charged poly (Diallyldimetheylammonium Chloride) (PDDA) followed by coating with Pd-Fe_3O_4 nanoparticle to get (Pd-Fe_3O_4/PDDA/COO--MWCNTs) composite. This composite was used for the determination of cholesterol by using Cholesterol Oxidase (ChOx) enzyme on Screen Printed Electrode (SPE). (Pd-Fe_3O_4/PDDA/COO--MWCNTs) composite provides biocompatible microenvironment for the ChOx to exhibit Direct Electron Transfer (DET) on electrode surface. A well defined redox peak at -0.365 and -0.443 V was observed, corresponding to the DET of the FAD/$FADH_2$ of ChOx. Enzyme modified SPE was characterized by cyclic voltammetry and electrochemical impedance spectroscopy by means of $Fe(CN)_6^{3-/4}$ as an electrochemical probe. The linear range of the enzyme modified SPE was found to be 10-80 µm (R=0.9972) with detection limit of 1 µm of cholesterol. The sensitivity of the enzyme modified SPE was found to be 10.45 $\mu A\ \mu M^{-1}\ cm^{-2}$ for the determination of cholesterol, common interferents such as ascorbic acid, uric acid and glucose did not cause any interference because of low operating potential.

Keywords: Pd-Fe_3O_4; Nanoparticles; Screen Printed Electrode; Cholesterol Oxidase

Introduction

Preparation of Biocompatible Palladium-Fe_3O_4 Nanoparticles/Multiwalled Carbon Nanotubes Composite and its Electrocatalytic Activity towards Determination of Cholesterol on Screen Printed Electrode

The magnetic nanoparticles in general, iron oxide (Fe_3O_4) have been attracted an increasing interest in the development of nanostructured materials and nanotechnology in biotechnology and medicine [1]. The main advantage of magnetic nanoparticles is that, they can easily and rapidly separate from their matrix by an external magnetic field. Some of the common features associated with the Fe_3O_4 nanoparticles are good biocompatibility, strong superparamagnetic property, high surface area, low toxicity and ease of preparation [2,3]. Thus, Fe_3O_4 nanoparticles have been used in a wide range of potential applications such as, electrochemical sensors/biosensors, catalysis, immunoassays, data storage [4-7]. Various methods have been used for the synthesis of magnetic nanoparticles which includes hydrothermal synthesis, co-precipitation, sol-gel method, microwave irradiation method [8-11]. The later method has significant advantage with respect to higher reaction rates and product yields in a shorter period of time.

Carbon nanotubes are one of the new kinds of carbon material, discovered in the last decades of the 20th century [12]. Researchers have explored various potential characteristics of CNTs, which could be applicable to various fields [13]. It was found that CNTs have excellent electronic conductivity, mechanical strength, chemical stability and unique structural properties [14]. However, the main drawbacks exist in the processibility of CNTs in solution, in which they precipitate into ropes or bundles

 ***Corresponding author email:** jsmelo@barc.gov.in, sureshssmrv@yahoo.co.in*

due to strong Van der Waals interactions [15]. To overcome this problem, surface modifications have been employed, such as chemical functionalization using strong acids, polymer wrapping of CNTs [16,17]. In later method i.e. chemical functionalization of CNTs using strong acid results in partial oxidation of the carbon atoms to produce oxygen containing groups such as carboxylic groups, especially in the open ends of CNTs [18]. These groups are negatively charged in the aqueous solution and can interact with positively charged poly electrolytes [19].

Cholesterol is one of the most important analyte in clinical analysis, because its assay is important for diagnosis and prevention of a numerous clinical disorders such as, hypertension, cerebral thrombosis, arteriosclerosis and coronary heart disease [20]. Recent studies explored that cholesterol plays a vital role in the brain synapses and also in the immune system including protection against cancer. In earlier days, cholesterol was determined by using non-enzymatic spectrophotometric techniques by using colored substances [21]. However, this technique suffers from low specificity, instability of reagents and high cost. These can be effectively addressed by using enzymatic cholesterol biosensor. Some of the advantages of enzymatic cholesterol biosensors are specificity, simplicity, rapidness and cost effectiveness [22]. The most commonly used enzyme for the construction of cholesterol biosensor is cholesterol oxidase. ChOx is a Flavin-Adenine-Dinucleotide (FAD) containing flavoenzyme. In the presence of oxygen, ChOx catalyzes two reactions; oxidation of cholesterol to cholest-5-en-3-one and subsequently the isomerization to cholest-4-en-3-one.

Direct electrochemistry of redox enzyme systems has gained increasing interest both for the study of the electron transport proteins as well as development of third generation reagent less electrochemical biosensors [23,24]. However, direct electron transfer between redox enzyme and electrode is generally difficult to observe due to several factors. Such as, enzyme active sites are deeply embedded in protein matrix, resulting in a long distance between active sites and underlying electrode. In addition, conformational changes or denaturation of redox enzyme often occur while immobilization of enzyme onto the electrode surface. Thus, to obtain DET, many techniques have been developed such as layer-by-layer technique, covalent binding using cross linkers, physical adsorption [25-27]. Physical adsorption method involves van der Waals forces, ionic binding or hydrophobic forces. The main advantage of this method is that it is simple and can be used under mild conditions. It requires only a minimum activation steps resulting in little or no conformational changes of the enzyme or destruction of its active centre [28].

In the present work, a simple and facile microwave method was adopted to prepare Fe_3O_4 and Pd- Fe_3O_4 nanoparticles by following the procedure given in the research article with slight modifications [29]. Formation of both Fe_3O_4 and Pd-Fe_3O_4 nanoparticles were confirmed by pXRD, TEM, EDX and FT-IR analysis. Negatively charged Pd- Fe_3O_4 nanoparticles were mixed with positively charged PDDA wrapped MWCNTs to get negatively charged novel composite. This negatively charged novel composite was drop casted on the Screen Printed Electrode (SPE). Positively charged ChOx (pH 4. 0) was immobilized on the composite by physical adsorption method. Enzyme modified screen printed electrode showed electrocatalytic activity towards detection of cholesterol. Cyclic Voltammery (CV) and Electrochemical Impedance Spectroscopy (EIS) techniques were used to characterize the enzyme modified screen printed electrode. Above mentioned novel composite provides biocompatible microenvironment for the ChOx to exhibit DET on SPE. To the best of our knowledge, for the first time we have used this novel composite for detection of cholesterol.

Methods

Reagents

TritonX-100,Cholesterol, $Pd(NH_3)4Cl_2 \bullet H_2O$, $FeSO_4 \bullet 7H_2O$, MWCNTs and PDDA (Mw: 200,000-350,000), were purchased from Sigma Aldrich. Cholesterol oxidase was procured from SRL, India. Screen printed electrodes of diameter 3 mm (0.071 cm^2) were purchased from CH instruments (product no. TE 100). Phosphate Buffer Saline of pH 7. 0 (PBS) was prepared from stock solutions of 0.1 M KH_2PO_4, 0.1 M K_2HPO_4 and 0.1M KCl. All other chemicals used were of analytical reagent grade unless otherwise mentioned and used without further purification. All solutions were prepared with milli-Q water.

Enzyme solution preparation

100 U/ml ChOx solution was prepared in 0.1 M acetate buffer solution of pH 4. A stock solution of 10 mM cholesterol was prepared by dissolving 0.0967 g of cholesterol in a mixture of 1 mL Triton X-100 and 0.5 mL isopropanol at 65°C and diluting the resulting solution to 25 mL in a standard flask using hot PBS of pH 7.0. The solution was stored at 4°C in the dark and was stable for two weeks (until a slight turbidity was observed).

Synthesis of Fe_3O_4 and Pd- Fe_3O_4 nanoparticles

As stated earlier, Fe_3O_4 and Pd- Fe_3O_4 nanoparticles were prepared according to the procedure described elsewhere [29]. In brief, 2.0 mm $FeSO_4.7H_2O$ was dissolved in 100 ml distilled water with continuous stirring. The pH of the solution was adjusted to 11 by conc. ammonia solution resulting in the formation of black precipitation. This suspension was transferred into microwave oven, in which microwave radiation of high energy was applied for one minute. The product Fe_3O_4 nanoparticles were separated by centrifugation method. Finally Fe_3O_4 nanoparticles washed thoroughly with water followed by ethanol and dried at 50°C in vacuum oven.

Similarly, Pd- Fe_3O_4 nanoparticles were prepared by co-precipitation method. 0.5 mm Pd $(NH_3)4Cl_2 \bullet H_2O$, and 2.0 mmol $FeSO_4 \bullet 7H_2O$ were dissolved in 100 ml distilled water with constant stirring. The pH of the solution was adjusted to about 11 by conc. ammonia solution. Then the reaction mixer was taken into microwave oven for microwave irradiation. The product was isolated by using above descried procedure.

Electrochemical measurements

Cyclic voltammetry, electrochemical impedance

spectroscopy, differential pulse voltammetry experiments were carried out with Versa stat 3 (Princeton Applied Research, USA). The microwave oven used in the present study was a domestic microwave oven (LG, intellowave, MS-2342 AE). Powder X-Ray Diffraction (pXRD) patterns of the samples were recorded using a Philips X'pert Pro diffractometer with CuKα (λ = 1.5418 Å). FT-IR experiments were carried out with Bruker Alpha-T FTIR spectrometer (ATR mode, diamond crystal, resolution 4 cm^{-1}, 400-4000 cm^{-1}). The morphology of the samples were analyzed by the Field emission scanning electron microscopy (Hitachi, S4800 FE-SEM) and the Field emission transmission electron microscopy (Hitachi, HF 3600 FE-TEM). TEM experiments were performed at an acceleration voltage of 300 kV. For the elemental mapping study, an Energy Dispersive X-Ray Spectroscopy (EDXS) connected to a TEM was used in scanning mode. TEM samples were prepared by dropping ultrasonically dispersed isopropyl alcohol solution of nanoparticles on a copper grid coated with amorphous carbon film. All experiments were done in an electrochemical cell consisting of SPE with an unmodified or modified carbon working electrode, a carbon counter electrode and Ag/AgCl reference electrode.

Preparation of enzyme modified screen printed electrode

As we already discussed in the introduction, CNTs are insoluble in most of the solvents because they precipitate into ropes are bundles due to strong Vander Waals interactions. To overcome this difficulty, we introduced carboxylic groups on MWCNTs surface by refluxing with conc. nitric acid for 5 h, followed by filtration and washed with pure water until the filtrate become neutral. Finally the product was dried in vacuum at 50°C [30]. PDDA is a water soluble, quaternary ammonium cationic polyelectrolyte. It is positively charged colloid when dissolved in aqueous solutions [31,32]. The positively charged PDDA polymer can be easily wrapped/coated on negatively charged MWCNTs [33]. 1 mg/ml carboxylated MWCNTs dispersed in 0.2% PDDA solution, ultrasonicalted for 20 min. followed by stirred at 50°C for 12 h. To this composite 0.5 mg/ml Pd- Fe_3O_4 nanoparticles were added and stirred for 12 h at room temperature. In this stage negatively charged Pd- Fe_3O_4 nanoparticles coated on positively charged MWCNTs wrapped with PDDA as shown in figure 1.

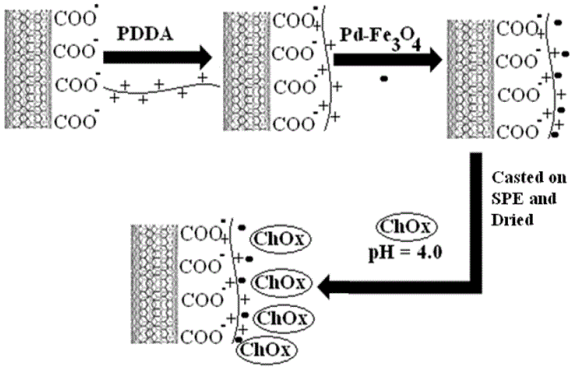

Figure 1: Schematic representation for the fabrication of enzyme electrode based on the ($PdFe_3O_4$/PDDA/COO--MWCNTs) composite.

2.5 µl of Pd- Fe_3O_4/PDDA/COO^--MWCNTs composite was drop casted on screen printed electrode, dried at ambient temperature. 5 µl of positively charged ChOx (pH 4.0) drop casted on composite, dried at 4°C. Hereafter, the enzyme modified electrode was denoted as ChOx-(Pd- Fe_3O_4/PDDA/COO^--MWCNTs)/SPE.

Results and discussion

Characterization of Fe_3O_4 and Pd- Fe_3O_4 nano particles using pXRD, TEM, EDX and FT-IR techniques

Figure 2a shows XRD patterns of the synthesized Fe_3O_4 nanoparticles. Diffraction peaks of Fe_3O_4 nanoparticles were obtained at 30.18°, 35.54°, 43.29°, 53.69°, 57.29° and 62.96° corresponding to the index planes (220), (311), (400), (422), (511) and (440) respectively. This is quite identical to pure Fe_3O_4 nanoparticles and well matched with that of JCPDS no. 82-1533. This revealed that the Fe_3O_4 nanoparticles have a cubic spinel structure [34,35]. Also, no characteristic peaks of impurities were observed. From the XRD data, the mean particle diameter of Fe_3O_4 nanoparticles was calculated from index planes (220), (311) and (400) by using Debye-Schererrer's equation, which is given below.)

$$D = 0.94\lambda / \beta \cos\theta \qquad (1)$$

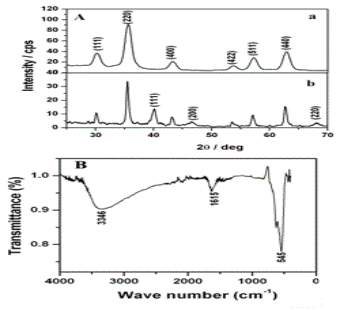

Figure 2: A. XRD patterns of Fe_3O_4 (a) and Pd- Fe3O4 (b) nanoparticles. B. FT-IR spectrum of Fe_3O_4 nanoparticles.

Where, λ- wavelength of X-ray, β- full width at half maximum,θ- Bragg's diffraction angle. The mean particle diameter of Fe_3O_4 nanoparticles was found to be 10 nm. These results depicts that the Fe_3O_4 nanoparticles can be rapidly synthesized with 5-10 minutes. Usually most of the Fe_3O_4 nanoparticles synthetic methods need more than an hour [36].

Formation of Fe_3O_4 nanoparticles by microwave irradiation can be explained as follows

$$Fe^{2+} + 2NH_3 + H_2O \rightarrow Fe(OH)_{2+} 2NH_4^+ \qquad (2)$$

When ammonia is added to the $FeSO_4$ solution $Fe(OH)_2$ is formed according to the equation 2, which is oxidized to Fe_3O_4 nanoparticles und the influence of microwave radiation as follows

$$3Fe(OH)_{2+} 1/2O_2 \xrightarrow{\text{Microwave Radiations}} Fe_3O_4 + 3H_2O \qquad (3)$$

Similarly figure 2b shows XRD patterns of the Fe_3O_4 nanoparticles decorated on Pd. The addition diffraction peaks at 40.07°, 46.54° and 68.09° corresponding to the (111), (2000) and (220) lattice planes were attributed to formation of Pd nanoparticles [37,38]. The mean particle diameter of Pd-Fe_3O_4 nanoparticles was found to 90 nm according to equation 1. The possible mechanism for the formation of Pd-Fe_3O_4 shown as below,

$$2\,Fe^{2+} + \left[Pd\,(NH_3)_4\right]^{+} + 2OH^{-} + 4H_2O \rightarrow 2\,Fe(OH)_3 + Pd + 4NH_4^{+} \quad (4)$$

$$Fe^{2+} + 2NH_3 + H_2O \xrightarrow[\text{Radiations}]{\text{Microwave}} Fe\,(OH)_{2+}\,2NH_4^{+} \quad (5)$$

$$2\,Fe\,(OH)_3 + Fe(OH)_2 + Pd \rightarrow Pd - Fe_3O_4 + 4H_2O \quad (6)$$

FT-IR data of Fe_3O_4 nanoparticles is shown in figure 2B. It is noteworthy that in figure 2B, peak at 545 cm^{-1} is attributed to the Fe-O bond vibration of Fe_3O_4 [39]. The broad peak at 3346 cm^{-1} is due to stretching vibrations of –OH bond, which is absorbed by Fe_3O_4 nano particles. Also, the peak at ~1610 cm^{-1} may be assigned to the deformation vibrations of water molecules trapped onto the magnetic nanoparticles [40]. These results confirm the formation of Fe_3O_4 nanoparticles. There was no major change in the FT-IR spectrum of Pd-Fe_3O_4 (results not shown).

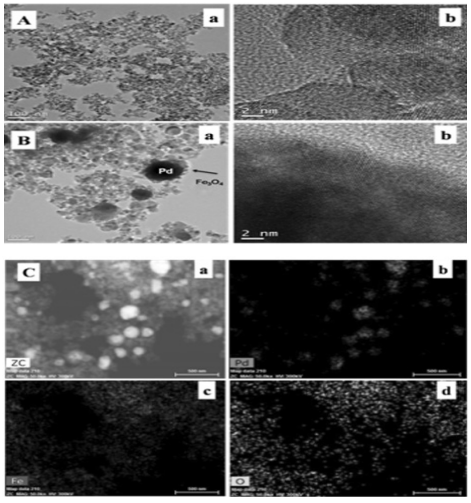

Figure 3: (a) TEM (b) HRTEM images of Fe_3O_4 nanoparticles. B. (a) TEM (b) HRTEM Images of Pd-Fe_3O_4 nanoparticles. C. (a) Bright field TEM image Pd-Fe_3O_4 nanoparticles, the corresponding EDX maps depict the distribution of constituting individual elements within the structure as shown in (b-d). The images correspond to the (b) Fe, (c) Pd, and (d) O.

Figure 3A, 3B shows TEM images of Fe_3O_4 and Pd-Fe_3O_4 nanoparticles respectively. Both Fe_3O_4 and Pd- Fe_3O_4 nanoparticles appeared to be almost spherical in shape. TEM image of figure 3B (a) clearly depicts the presence of slightly bigger Pd nanoparticles (dark contrast) surrounded by Fe_3O_4 nanoparticles, which is evidenced in the difference in contrast. The average diameter of Fe_3O_4 nanoparticles was found to be 12.8 nm, whereas, the average particle size of Pd- Fe_3O_4 nanoparticles was found to be 92.4 nm. These results are in well agreement with XRD results shown in figure 3A. The high resolution TEM (HRTEM) images of Fe_3O_4 and Pd-Fe_3O_4 nanoparticles are shown in figure 3A (b) & 3B (b), respectively. The distance between two lattice planes of the Fe_3O_4 crystallite was 0.252 nm, which corresponds to the (311) plane of spinal Fe_3O_4. In the same way, HRTEM image of Pd- Fe_3O_4 nanoparticle showed well resolved lattice fringes with a distance of 0.225 nm, corresponding to the (111) plane of cubic Pd. Furthermore, the presence of Pd nanoparticles in Fe_3O_4 was also confirmed using scanning transmission electron microscope (STEM) coupled with elemental mapping analysis (STEM-EDS). Figure 3C (a) shows a bright field TEM image of Pd-Fe_3O_4 nanoparticles. The corresponding elemental maps are given in figure 3C (b-d). The EDS mapping results suggest that metallic Pd core is surrounded by several Fe_3O_4 nanoparticles.

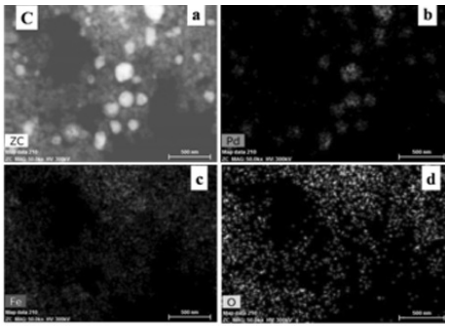

Figure 4: SEM images of unmodified SPE (a), (PDDA/COO^--MWCNTs)/SPE (b), (Pd-Fe_3O_4/PDDA/COO^--MWCNTs)/SPE(c)andChOx-(Pd-Fe_3O_4/PDDA/COO--MWCNTs)/SPE (d).

Figure 4 displays the SEM images of unmodified SPE (a), (PDDA/COO^--MWCNTs)/SPE (b), (Pd-Fe_3O_4/PDDA/COO^--MWCNTs)/SPE (c) and ChOx-(Pd- Fe_3O_4/PDDA/COO^--MWCNTs)/SPE (d). The morphology of the unmodified SPE exhibits rough surface having different size grains of several microns. PDDA coated MWCNTs composite is uniformly deposited on SPE, which can be seen in image (b). Nano sized Pd-Fe_3O_4 particles appear as small white grains which are incorporated into (PDDA/COO^--MWCNTs) composite clearly visible in image (c). Image (d) shows uniform immobilization of ChOx enzyme on (Pd-Fe_3O_4/PDDA/COO^--MWCNTs) composite. Inset shows the different size granules of ChOx enzyme.

Characterization of ChOx-(Pd- Fe_3O_4/PDDA/COO^--MWCNTs)/SPE using CV and EIS

$Fe(CN)_6^{3-/4-}$ redox couple is widely used as an electrochemical probe to characterize the property of unmodified/modified electrodes. Figure 5

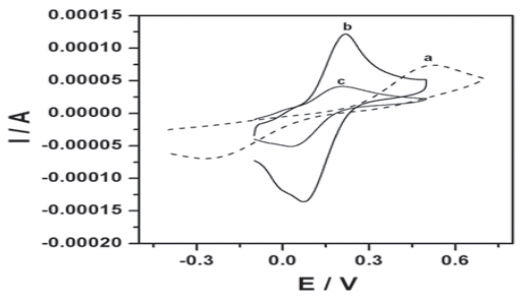

Figure 5: Cyclic voltammograms of unmodified SPE (a), Pd- Fe3O4/PDDA/COO--MWCNTs)/SPE (b) and ChOx-(Pd- Fe_3O_4/PDDA/COO--MWCNTs)/SPE (c) in 0.1 M PBS containing 5 mM $Fe(CN)6^{4-/3-}$ (pH 7.0); scan rate: 50 mVs-1.

Illustrates, the cyclic volt ammogramms of SPE, (Pd-Fe_3O_4/PDDA/COO^--MWCNTs)/SPE and ChOx-(Pd-Fe_3O_4/PDDA/COO^--MWCNTs)/SPE in 5 mM $Fe(CN)_6^{3-/4-}$ containing PBS (pH 7.0) at scan rate of 50 mVs^{-1}. Irreversible voltammogram was observed at SPE (curve a, dotted line) with minimal cathodic peak current (Ipc) and anodic peak current (Ipa). The cathodic peak potential (Epc) and anodic peak potential (Epa) were found at 521 mV and -256 mV respectively with peak to peak separation (ΔEp) 777 mV. However, SPE modified with (Pd-Fe_3O_4/PDDA/COO^--MWCNTs) composite, a well redox peak of $Fe(CN)_6^{3-/4-}$ with the ΔEp 48 mV (curve b) was obtained. These results depict that the over potential decreased by 729 mV and around 2 fold of increase in current was observed for 5 mM $Fe(CN)_6^{3-/4-}$ at (Pd- Fe_3O_4/PDDA/COO^--MWCNTs)/SPE than that of SPE. This shows that Electrocatalytic activity of (Pd- Fe_3O_4/PDDA/COO^--MWCNTs) composite. After immobilization of ChOx enzyme on (Pd- Fe_3O_4/PDDA/COO^--MWCNTs)/SPE, decreased in peak current was observed (curve c). This could be attributed to macromolecular non conducting enzymatic structure, impede electrochemical redox reaction of $Fe(CN)_6^{3-/4-}$ at electrode surface. This demonstrates that ChOx enzyme successfully immobilized on (Pd- Fe_3O_4/PDDA/COO^--MWCNTs) composite by means of electrostatic attraction.

Elctrochemical Impedance Spectroscopy (EIS) is a powerful and sensitive characterization tool for studying the charge transfer process at electrode/electrolyte interface [41]. Hence, Characterization of SPE, (Pd- Fe_3O_4/PDDA/COO^--MWCNTs)/SPE and ChOx-(Pd- Fe_3O_4/PDDA/COO^--MWCNTs)/SPE was further investigated using EIS. EIS was carried out in the presence of 5 mM Fe $(CN)6^{4-/3-}$as a electrochemical redox probe, in the frequency range of 100 kHz to 0.1 Hz with amplitude of 5 mV as shown in figure 6A The equivalent circuit shown in the inset of figure 6B was used to fit experimental data. The simulated curve of experimental data and best fitting equivalent circuit are shown in the figure 6C. The obtained impedance data are shown in Table 1.

The circuit includes the solution resistance (Rs), charge transfer resistance (Rct), double layer capacitance (Qdl), Warburg impedance (Zw), Faradaic resistance, (Rf) and Faradaic capacitance (Cf). At SPE, big semicircle having a Rct of 5714 Ω was observed for $Fe(CN)6^{4-/3-}$ (curve a), which suggests that unmodified SPE exhibits sluggish and unfavorable $Fe(CN)6^{4-/3-}$ electron transfer. However, SPE modified with (Pd- Fe_3O_4/

Table 1: EIS data of unmodified SPE, (Pd- Fe_3O_4/PDDA/COO--MWCNTs)/SPE and ChOx-(Pd- Fe_3O_4/PDDA/COO--MWCNTs)/SPE in 5 mM $Fe(CN)_6^{3-/4}$

Electrode	R_s/Ω	n	Q/μF	R_{ct}/Ω	W/Ω
SPE	189	0.95	0. 49	5714	0.0009
Pd- Fe_3O_4/PDDA/COO^--MWCNTs)/SPE	198	0.97	0. 23	0.19	0.006
ChOx-(Pd- Fe_3O_4/PDDA/ COO^--MWCNTs)/SPE	196	0.78	14.5	557	0.0016

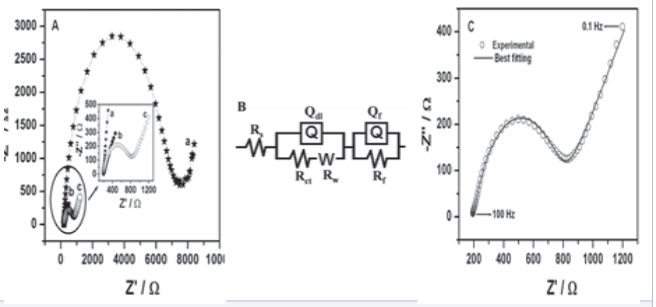

Figure 6: Nyquist impedance plots of unmodified SPE (a), Pd- Fe_3O_4/PDDA/COO--MWCNTs)/SPE (b) and ChOx-(Pd- Fe_3O_4/PDDA/COO--MWCNTs)/SPE (c) in 0.1 MPBS containing 5 mM $Fe(CN)_6^{4-/3-}$ (pH 7.0). The frequency range is from 100 kHz to 0.1 Hz and amplitude 5 mV. B. The equivalent circuit used to fit experimental data. (C) Nyquist impedance plots of experimental data of ChOx-(Pd-Fe_3O_4/PDDA/COO--MWCNTs)/SPE and best fitting by using equivalent.

PDDA/COO^--MWC) composite, big semicircle was replaced with straight line, which have a Rct of 0.19 Ω as shown in figure 5A inset (curve b). This shows (Pd- Fe_3O_4/PDDA/COO^--MWCNTs) composite facilitates fast and favorable electron transfer towards electrode surface. Small semicircle was observed (curve c) with a Rct of 557 Ω, when ChOx enzyme immobilized on (Pd- Fe_3O_4/PDDA/COO^--MWCNTs)/SPE, which illustrates that non conducting macromolecular ChOx was successfully immobilized modified SPE and it oppose the electron transfer towards electrode surface.

Direct electrochemistry of ChOx on (Pd- Fe_3O_4/PDDA/COO^--MWCNTs)/SPE

Figure 7 shows, cyclic voltammogram of ChOx on unmodified SPE (curve a) and (Pd- Fe_3O_4/PDDA/COO^--MWCNTs)/SPE (curse b). When ChOx immobilized on unmodified SPE, which does not facilitate DET. This illustrates that unmodified SPE does not provide micro environment for the immobilization of ChOx. However, ChOx immobilized on (Pd-Fe_3O_4/PDDA/COO^--MWCNTs)/SPE exhibits a pair of well defined redox peaks at

-0.365 and -0.443, these peaks are assigned for FAD/$FADH_2$, which could be ascribed to electron transfer between ChOx and under laying electrode [19,22,27]. The potential difference between the two peaks ΔEp was 78

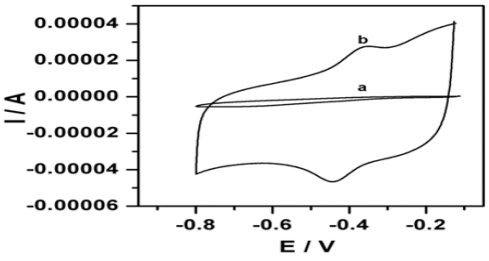

Figure 7: Cyclic voltammograms of ChOx-unmodified SPE (a) and ChOx-(Pd-Fe_3O_4/PDDA/COO--MWCNTs)/SPE in 0.1M PBS (pH 7.0) scan rate: 50mVs-1.

mV at a scan rate of 50 mVs^{-1}, which suggests that ChOx has undergone a quasi-reversible redox reaction (Pd-Fe_3O_4/PDDA/COO^--MWCNTs)/SPE. The surface area (τ) of ChOx-(Pd-Fe_3O_4/PDDA/COO^--MWCNTs)/SPE was calculated using the following equation.

$$\tau = \frac{Q}{nFA} \qquad (7)$$

Where, Q is the charge, n is the number of electrons transferred, *F* is the Faraday constant. Therefore (τ) was found to be 5.38 × 10^{-9} mol cm^{-2}.

Effect of scan rate and pH at ChOx-(Pd-Fe_3O_4/PDDA/COO^--MWCNTs)/SPE

To determine the kinetics of electrode reactions, the effect of scan rate on the voltammetric response of ChOx-(Pd-Fe_3O_4/PDDA/COO^--MWCNTs)/SPE in a 0.1 M PBS of pH 7 was studied in the range of 5-75 mVs^{-1} as shown in figure 8A. The linear regression equations are as given below

Ipa = -6.6628E-7 + 5.4642E-7 ν (Vs^{-1}); R = 0.9981 (8)

Ipc = -1.4345E-5 - 6.3799E- 7 ν (Vs^{-1}); R = 0.9932 (9)

The redox peak current of ChOx increased linearly with increasing scan rate (Figure 8B) and the peak to peak separation also increased, indicating that surface controlled quasi-reversible process is involved.

In addition, the anodic peak potential shifted to a more potential value with increasing scan rate, where as the cathodic peak potential shifted in a negative direction. The pH of the electrolyte solution has a significant influence on the redox reaction of FAD/$FADH_2$ of ChOx with respect to peak current and peak potential. Figure 9A Shows cyclic voltammograms of effect of pH of electrolyte in the range 4 to 8 studied on the response of ChOx-(Pd-Fe_3O_4/PDDA/COO^--MWCNTs)/SPE. The electrochemical response of enzyme immobilized on the electrode surface is due to redox reaction of its active site, i.e. FAD/$FADH_2$. Where, FAD is known to undergo redox reaction involving two electrons with two protons to form $FADH_2$.

The redox peak current of ChOx increased linearly with increasing scan rate (Figure 8B) and the peak to peak separation also increased, indicating that surface controlled quasi-reversible process is involved.

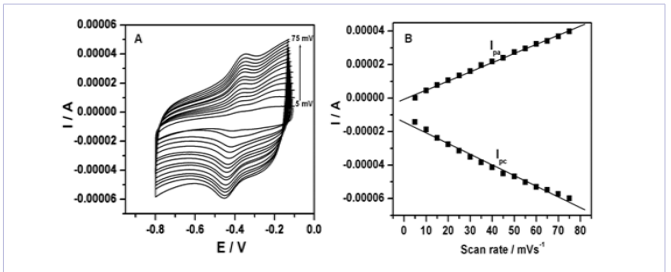

Figure8: Cyclic voltammograms of ChOx-(Pd- Fe_3O_4/PDDA/COO--MWCNTs)/SPE in PBS (pH 7.0) at different scan rates: (5-75 mV-1). B. The plot of peak current vs. scan rate.

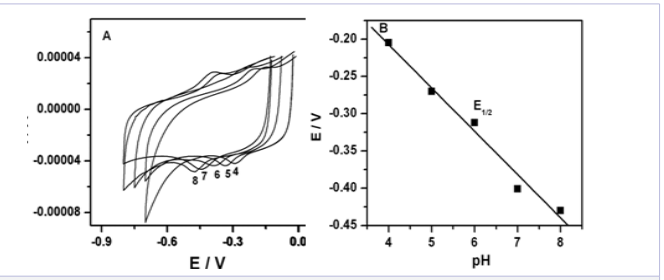

Figure 9: Cyclic voltammograms of ChOx-(Pd- Fe_3O_4/PDDA/COO--MWCNTs)/SPE at various pHs of the solution (pH 4–8) scan rate: 50mVs-1. (B) Plots of potential vs. $E_{1/2}$ at pH (4–8).

Due to protons involve in the reaction, the acidity of the solution has a significant effect on the redox potential of ChOx. Thus, the anodic and cathodic peak potentials of ChOx immobilized on the (Pd-Fe_3O_4/PDDA/COO^--MWCNTs)/SPE should be pH dependent. It was observed that, redox peak potential of the enzyme shifted towards negative with increase in pH as shown in figure 8B indicating that protons are involved in the redox reaction. A good linear relationship was obtained between half wave potential (E1/2) and the solution pH. The corresponding linear regression equation is given as

$E_{1/2}$ = -0.025 - 0.058 pH; R = 0.9908 (10)

From the above equation, slope of $E_{1/2}$ is 58 mV, which is close to the theoretical value (59 mV pH^{-1}) for a classical Nernstian two electrons and protons process. Hence, ChOx redox system is a two proton participated two electron redox processes.

Determination of cholesterol based on the direct electrochemistry of ChOx on the (Pd-Fe_3O_4/PDDA/COO^--MWCNTs)/SPE

In the this protocol, the direct electrochemistry of ChOx is based on the redox reaction of its active center, i.e. FAD, in the absence of oxygen, direct electron transfer of immobilized ChOx can be expressed as follows.In the presence of oxygen, the reduced enzyme is oxidized very quickly at the electrode surface. Electron transfer turnover rate of the molecular oxygen is about 700 s^{-1} to

accept electrons [42]. This is much faster than that of ChOx on

$$ChOx-FAD+2H^{+}+2e^{-} \leftrightarrow ChOx-FADH_2 \quad (11)$$

the (Pd-Fe_3O_4/PDDA/COO^--MWCNTs)/SPE. As a result, obvious electrostatic process towards the reduction of dissolved oxygen, which is given below

$$ChOx-FADH_2+O_2 \rightarrow ChOx-FAD+H_2O_2 \quad (12)$$

The catalytic regeneration of the enzyme in its oxidized form causes the loss of reversibility as a result increase in the size of the reduction peak as shown in figure 10 (curve b) [24].

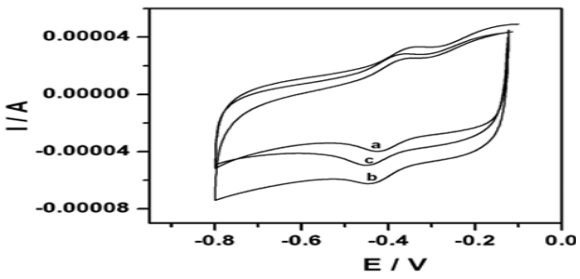

Figure 10: Cyclic voltammograms obtained at ChOx-(Pd- Fe_3O_4/PDDA/COO—MWCNTs)/SPE in nitrogen saturated and oxygen saturated PBS (a and b), after addition of 50 µM cholesterol to oxygen saturated PBS (c). Scan rate: 50mVs-1.

By the addition of cholesterol, a competitive reaction take place at the vicinity of the enzyme modified electrode surface. Thus, leading to the decrease of reduction peak current (curve c), as a result the sensitive determination of cholesterol. In other words, in the presence of oxygen, ChOx on modified electrode will catalyze the oxidation of cholesterol according to the following enzymatic reaction.

$$ChOx-FAD+Cholesterol \rightarrow ChOx-FADH_2+Choles-4-en-3-one \quad (13)$$

The reduction peak of the ChOx-(Pd-Fe_3O_4/PDDA/COO^--MWCNTs)/SPE in oxygen saturated PBS (pH 7. 0), decreased with addition of cholesterol, which suggested that the immobilized ChOx still retained its enzymatic activity. This could be due to the biocompatible, microenvironment provided by (Pd-Fe_3O_4/PDDA/COO^--MWCNTs) composite. Thus, the addition of cholesterol restrains Electrocatalytic reaction between the oxidized form of ChOx i.e. ChOx-FAD and cholesterol, which attenuates the concentration of the ChOx-FAD. This causes decrease in the reduction peak current of the enzyme [27]. Also, the dissolved oxygen mediates the enzymatic oxidation of cholesterol by ChOx. Therefore, the depletion of the oxygen proximal to the electrode surface makes the reduction of the oxidized form of ChOx less favorable, leading to the decrease of the reduction peak current of the enzyme [43].

Eventually, cholesterol is determined by measuring the decreased reduction peak current, by the addition of cholesterol in oxygen saturated PBS (pH 7.0).

Figure 11A shows the differential pulse voltammograms of various cholesterol concentrations at ChOx-(Pd-Fe_3O_4/PDDA/COO^--MWCNTs)/SPE in oxygen saturated PBS (pH 7. 0). The reduction current decreased gradually upon increasing cholesterol concentration.

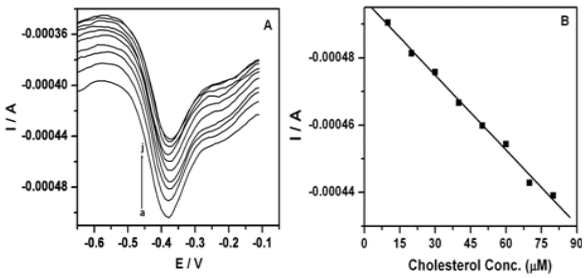

Figure11: Differential pulse voltammetric measurements at ChOx-(Pd- Fe_3O_4/PDDA/COO-MWCNTs)/SPE at oxygen saturated PBS(pH 7.0), without cholesterol (a) and (b–j) with cholesterol of 10, 20, 30, 40, 50, 60, 70, 80 and 90 µM. DPV parameters; scan rate: 20 mV s–1, pulse height: 200 mV, pulse width: 0.05 s, step height: 10 mV and step width:0.5 s. B. shows relationship between Ipc and concentrations of cholesterol.

Figure 11B shows the calibration current corresponding to decrease of reduction current and concentration of cholesterol. The linear regression equation is given by

Ipc (Cholesterol) (µA) = -4.9712E-4 + 7.4202E-7 C (Cholesterol) (µA); R = -0.9972 ..... (14)

Using slope of the above equation, the sensitivity of the enzyme modified SPE was calculated to be 0.742 µA μM^{-1} or 10.45 µA μM^{-1} cm^{-2} (area of electrode surface is 0.071 cm^2). Comparison of the enzyme modified SPE with other cholesterol determination based on SPEs are given in Table 2 [44-46].

Results shown in table 2, depicts that the sensitivity of the ChOx-(Pd-Fe_3O_4/PDDA/COO^--MWCNTs)/SPE much better when compare to other determinationofcholesterol based on SPEs. Furthermore, applied potential and detection limit of the ChOx-(Pd-Fe_3O_4/PDDA/COO^--MWCNTs)/SPE is quiet comparable with respect to other determination of cholesterol based on SPEs.

Table 2: Comparison of the ChOx enzyme SPE with other ChOx basedSPEs

Cholesterol Biosensor	Sensitivity µA μM^{-1}	Potential applied (mV)	Linear range (µM)	Detection limit (µM)	Reference
GNS-nPt/SPE	-	400	0-35	0.2	[44]
SP-rhodium-graphite--Au-P450scc	0.13	-400	10-70	-	[45]
SP-RP450scc	0.0138	-600	50-300	-	[46]
ChOx-(Pd-Fe_3O_4/PDDA/COO^--MWCNTs)/SPE	0.742	-380	10-80	1	Present work

Stability and reproducibility of the ChOx-(Pd-Fe_3O_4/PDDA/COO^--MWCNTs)/SPE

Direct electron transfer of ChOx on (Pd-Fe_3O_4/PDDA/COO^--MWCNTs)/SPE is very stable. When twenty consecutive CV curves obtained at ChOx-(Pd-Fe3O4/PDDA/COO^--MWCNTs)/SPE in 0.1 M PBS pH 7.0 at scan rate of 50mVs^{-1}, there was no change in the peak to peak separation. However, peak current gradually decreased. The electrode retained 86.6% of its initial response after twenty consecutive cycles. These results shows that ChOx binds strongly on (Pd-Fe_3O_4/PDDA/COO^--MWCNTs) composite. To ascertain fabrication reproducibility, five sets of ChOx on (Pd-Fe_3O_4/PDDA/COO^--MWCNTs)/SPE were fabricated for the determination of cholesterol. The results show that the enzyme modified SPE had satisfying reproducibility with the Relative Standard Deviation (RSD) of 9.5%.

Conclusion

Fe3O4 and Pd-Fe_3O_4nanoparticles were synthesized by simple and facile microwave method. Formation of $Fe_3O_4$and Pd- Fe_3O_4 nanoparticles were confirmed from powder X-ray diffraction and FT-IR techniques. Pd- Fe_3O_4 nanoparticles used for the preparation of biocompatible composite which consists of negatively charged mutliwalled carbon nanotubes (COO^--MWCNTs) wrapped with positively charged poly diallyldimethyl ammonium chloride. This composite was successfully used for the determination of cholesterol by using cholesterol oxidase enzyme on screen printed electrode. DET of ChOx was observed on (Pd- Fe_3O_4/PDDA/COO^--MWCNTs) composite which shows that the composite provides biocompatiable microenvironment for the ChOx. The linear range of the enzyme modified SPE was found to be 10-80 µM (R=9972) with detection limit of 1 µM. Common interferents such as ascorbic acid, uric acid and glucose did not cause any interference because of low operating potential.

Acknowledgements

The authors gratefully acknowledge the financial support from Vision Group on Science and Technology, Government of Karnataka. R. Manjunatha thanks Council of Scientific and Industrial Research, New Delhi for the award of Senior Research Fellowship. We thank Sri. A. V. S. Murthy, honorary secretary, Rashtreeya Sikshana Samiti Trust, Bangalore for his continuous support and encouragement.

References

1.Dresco PA, Zaitsev VS, Gambino RJ, Chu B. Preparation and Properties of Magnetite and Polymer Magnetite Nanoparticles. Langmuir. 1999;15(6):1945-1951. doi: 10.1021/la980971g

2.Teymourin H, Salimi A, Hallaj R. Low potential detection of NADH based on Fe_3O_4nanoparticles/multiwalled carbon nanotubes composite: Fabrication of integrated dehydrogenase-based lactate biosensor. Biosens Bioelectron. 2012;33(1):60-68. doi: 10.1016/j.bios.2011.12.031

3.Koneracka M, Kopcansky P, Antalik M, Timko M, Ramchand CN, Lobo D, et al. Immobilization of proteins and enzymes to fine magnetic particles. J Magn Magn Mater. 1999;201:427-430. doi: 10.1016/S0304-8853(99)00005-0

4.Zhang L, Zhai Y, Gao N, Wen D, Dong, S. Sensing H2O2 with layer-by-layer assembled Fe_3O_4–PDDA nanocomposite film. Electrochem Commun. 2008;10(10):1524-1526. doi: 10.1016/j.elecom.2008.05.022

5.Kassaee MZ, Masrouri H, Movahedi F. Sulfamic acid-functionalized magnetic Fe_3O_4 nanoparticles as an efficient and reusable catalyst for one-pot synthesis of α-amino nitriles in water. Appl Catal A: Gen. 2011;395(1-2):28-33. doi: 10.1016/j.apcata.2011.01.018

6.Wang SF, Tan YM. A novel amperometric immunosensor based on Fe_3O_4 magnetic nanoparticles/chitosan composite film for determination of ferritin. Anal Bioanal Chem. 2007;387(2):703-708. doi: 10.1007/s00216-006-0976-2

7.Service RF. Nanocrystals May Give Boost to Data Storage. Science. 2000;287(5460):1902-1903. doi: 10.1126/science.287.5460.1902

8.Li Y, Liao H, Qian Y. Hydrothermal Synthesis of Ultrafine α-Fe2O3 and Fe_3O_4Powders. Mater Res Bull. 1998;33(6):841-844. doi: 10.1016/S0025-5408(98)00055-5

9.Valenzuela R, Fuentes MC, Parra C, Baeza J, Duran N, Sharma SK, et al. Influence of stirring velocity on the synthesis of magnetite nanoparticles (Fe_3O_4) by the co-precipitation method. Alloys Compd. 2009;488(1):227-231. doi: 10.1016/j.jallcom.2009.08.087

10.Tang NJ, Zhong W, Jiang HY, Wu XL, Liu W, Du YW. Nanostructured magnetite (Fe_3O_4) thin films prepared by sol–gel method. J Magn Magn Mater. 2004;282:92-95. doi: 10.1016/j.jmmm.2004.04.022

11.Miao F, Hua W, Hu L, Huang K. Magnetic Fe_3O_4nanoparticles prepared by a facile and green microwave-assisted approach. Mater Lett. 2011;65(6):1031-1033. doi: 10.1016/j.matlet.2010.12.037

12.Decher G. Fuzzy Nanoassemblies: Toward Layered Polymeric Multicomposites. Science. 1997;277(5330):1232-1237. doi: 10.1126/science.277.5330.1232

13.Dyke CA, Tour JM. Solvent-Free Functionalization of Carbon Nanotubes. J Am Chem Soc. 2003;125(5):1156-1157. doi: 10.1021/ja0289806

14.Ajayan PM. Nanotubes from Carbon. Chem Rev. 1999;99(7):1787-1800.

15.Britz DA, Khlobystov AN. Noncovalent interactions of molecules with single walled carbon nanotubes Chem. Soc Rev. 2006;35:637-659. doi: 10.1039/B507451G

16.Esumi K, Ishigami M, Nakajima A, Sawada K, Honda H. Carbon. 1996;34:279.

17.Manjunatha R, Suresh GS, Melo JS, D'Souza SF, Venkatesha TV. Simultaneous determination of ascorbic acid, dopamine and uric acid using polystyrene sulfonate wrapped multiwalled carbon nanotubes bound to graphite electrode through layer-by-layer technique. Sens Actuators B. 2010;145(2):643-650. doi: 10.1016/j.snb.2010.01.011

18.Zhang J, Zou H, Qing Q, Yang Y, Li Q, Liu Z, et al. Effect of Chemical Oxidation on the Structure of Single-Walled Carbon Nanotubes. J Phys Chem B. 2003;107(16):3712-3718. doi: 10.1021/jp027500u

19.Manjunatha R, Nagaraj DH, Suresh GS, Melo JS, D'Souza SF, Venkatesha TV. Direct electrochemistry of cholesterol oxidase on MWCNTs. J Electroanal Chem. 2011;651(1):24-29.

20.MacLachlan J, Wotherspoon ATL, Ansell RO, Brooks CJW. Cholesterol oxidase: sources, physical properties and analytical applications. J Stedroid Biochem Mol Biol. 2000;72(5):169-195.

21.Richmond W. Preparation and Properties of a Cholesterol Oxidase from Nocardia sp. and Its Application to the Enzymatic Assay of Total Cholesterol in Serum. Clin Chem. 1973;19(12):1350-1356.

22.Basu AK, Chattopadhyay P, Roychoudhuri U, Chakraborty R. Development of cholesterol biosensor based on immobilized cholesterol esterase and cholesterol oxidase on oxygen electrode for the determination of total cholesterol in food samples. Bioelectro chemistry. 2007;70(2):375-379. doi: 10.1016/j.bioelechem.2006.05.006

23.Zhang J, Feng M, Tachikawa H, Layer-by-layer fabrication and direct electrochemistry of glucose oxidase on single wall carbon nanotubes. Biosens Bioelectron. 2007;22(12):3036-3041. doi: 10.1016/j.bios.2007.01.009

24.Zhang W, Li G. Third-Generation Biosensors Based on the Direct Electron Transfer of Proteins. Anal Sci. 2004;20(4):603-609. doi: 10.2116/analsci.20.603

25.Manjunatha R, Nagaraj DH, Suresh GS, Melo JS, D'Souza SF, Venkatesha TV. Electrochemical detection of acetaminophen on the functionalized MWCNTs modified electrode using layer-by-layer technique. Electrochem Acta. 2011;56(19):6619–6627.

26.Manjunatha R, Suresh GS, Melo JS, D'Souza SF, Venkatesha TV. An amperometric bienzymatic cholesterol biosensor based on functionalized graphene modified electrode and its electrocatalytic activity towards total cholesterol determination. Talanta. 2012;99(15):302-309. doi: 10.1016/j.talanta.2012.05.056

27.Li XR, Xu JJ, Chen HY. Potassium-doped carbon nanotubes toward the direct electrochemistry of cholesterol oxidase and its application in highly sensitive cholesterol biosensor. Electrochim Acta. 2011;56(25):9378-9385.

28.Arya SK, Datta M, Malhotra BD. Recent advances in cholesterol biosensor. Biosens Bioelectron. 2008;23(7):1083-1100. doi: 10.1016/j.bios.2007.10.018

29.Zheng B, Zhang M, Xiao D, Jin Y, Choi MMF. Fast microwave synthesis of Fe_3O_4 and Fe_3O_4/Ag magnetic nanoparticles using Fe2+ as precursor. Inorg Mater. 2010;46(10):1106-1111. doi: 10.1134/S0020168510100146

30.Itoh H, Sugimoto T. Systematic control of size, shape, structure, and magnetic properties of uniform magnetite and maghemite particles. J Colloid Interface Sci. 2003;265(2):283–295.

31.Sun J, Zhou S, Hou P, Yang Y, Weng J, Li X, Li M. Synthesis and characterization of biocompatible Fe_3O_4 nanoparticles. J Biomed Mater Res Part A. 2006;80(2):333-341. doi: 10.1002/jbm.a.30909

32.Eguílaz M, Villalonga R, Yanez-Sedeno P, Pingarron JM. Designing Electrochemical Interfaces with Functionalized Magnetic Nanoparticles and Wrapped Carbon Nanotubes as Platforms for the Construction of High-Performance Bienzyme Biosensors. Anal Chem. 2011;83(20):7807–7814. doi: 10.1021/ac201466m

33.Zhao H, Ju H. Multilayer membranes for glucose biosensing via layer-by-layer assembly of multiwall carbon nanotubes and glucose oxidase. Anal Biochem. 2006;350(1):138–144.

34.Guo M, Chen J, Li J, Nie L, Yao S. Carbon Nanotubes-Based Amperometric Cholesterol Biosensor Fabricated Through Layer-by-Layer Technique. Electroanalysis. 2004;16(23):1992-1998. doi: 10.1002/elan.200403053

35.Ran XQ, Yuan R, Chai YQ, Hong CL, Qian XQ. A sensitive amperometric immunosensor for alpha-fetoprotein based on carbon nanotube/DNA/Thi/nano-Au modified glassy carbon electrode. Colloids Surf B: Biointerfaces. 2010;79(2):421–426. doi: 10.1016/j.colsurfb.2010.05.012

36.Hu H, Yang H, Huang P, Cui D, Peng Y, Zhang J. et al. Unique role of ionic liquid in microwave-assisted synthesis of mono disperse magnetite nanoparticles. Chem Common. 2010;46:3866-3868. doi: 10.1039/B927321B

37.Yu Y, Zhao Y, Huang T, Liu H. Shape-controlled synthesis of palladium nano crystals by microwave irradiation. Pure Appl Chem. 2009;81(12):2377–2385. doi: 10.1351/PAC-CON-08-11-22

38.Navaladian S, Viswanathan B, Varadarajan TK, Viswanath RP. A Rapid Synthesis of Oriented Palladium Nanoparticles by UV Irradiation. Nanoscale Res Lett. 2009;4:181–186. doi: 10.1007/s11671-008-9223-4

39.Ma M, Zhang Y, Yu W, Shen HY, Zhang HQ, Gu N. Preparation and characterization of magnetite nanoparticles coated by amino silane. Colloids and Surf A: Physicochem Eng Aspects. 2003;212(2-3):219–226. doi: 10.1016/S0927-7757(02)00305-9

40.Racuciu M, Creanga DE, Airinei A, Chicea D, Badescu V. Synthesis and properties of magnetic nanoparticles coated with biocompatible compounds. Mat Sci Poland. 2010;28(3):609-616.

41.Chen H, Heng CK, Puiu PD, Zhou XD, Lee AC, Lim M, et al. Detection of Saccharomyces cerevisiae immobilized on self-assembled monolayer (SAM) of alkanethiolate using electrochemical impedance spectroscopy. Anal Chim Acta. 2005;554(1-2):52-59.

42.Xiao Y, Patolsky F, Katz E, Hainfeld JF, Willner I. "Plugging into Enzymes": Nanowiring of Redox Enzymes by a Gold Nanoparticle. Science. 2003;299(5614):1877-1881. doi: 10.1126/science.1080664

43.Zhang W, Huang Y, Dai H, Wang X, Fan C, Li G. Tuning the redox and enzymatic activity of glucose oxidase in layered organic films and its application in glucose biosensors. Anal Biochem. 2004;329(1):85-90. doi: 10.1016/j.ab.2004.01.032

44.Dey RS, Raj CR. Development of an Amperometric Cholesterol Biosensor Based on Graphene−Pt Nanoparticle Hybrid Material. J Phys Chem C. 2010;114(49):21427-21433. doi: 10.1021/jp105895a

45.Shumyantseva V, Deluca G, Bulko T, Carrara S, Nicolini C, Usanov SA, et al. Cholesterol amperometric biosensor based on cytochrome P450scc. Biosen Bioelectron. 2004;19(9):971-6. doi: 10.1016/j.bios.2003.09.001

46.Shumyantseva VV, Carrara S, Bavastrello V, Riley DJ, Bulko TV, Skryabin KG, et al. Direct electron transfer between cytochrome P450scc and gold nanoparticles on screen-printed rhodium–graphite electrodes. Biosen Bioelectron. 2005;21(1):217-222. doi: 10.1016/j.bios.2004.10.008